Radial Pressure Distributions in an Air-Riding Face Seal

Amir Ibrahim, David Gillespie, Department of Engineering Science, University of Oxford, Oxford, United Kingdom, John Garratt, Rolls-Royce, Derby, United Kingdom

Long Abstract

Introduction

Shaft seals are found wherever rotating and stationary components are in close proximity and flow must be restricted in the gas turbine. There may be as many as 50 installed seals in a jet engine [1]. Two main categories of seals are typically used; air-to-oil seals and air-to-air seals. The former type are bearing sump seals that restrict leakage from a high pressure region into the bearing compartments. The compressor and turbine interstage seals are classified as air-to-air seals. They are the primary means of metering cooling airflow at a range of pressures to provide the necessary cooling air to the turbine blades and vanes and also preventing gas recirculation [2]. In the secondary air system, conventional face seals have been considered as potential replacements for labyrinth seals in an attempt to reduce leakage rates and reduce wear through non-contact operation [3]. Although they exhibit significantly lower leakage rates than labyrinth seals their operation is limited to lower pressure differentials and temperatures [4]. Non-contacting face seals rely on high pressures induced in a thin air film between stationary and rotating faces. They offer ultra-low leakage and very low wear compared to contacting seals in aircraft engines. Large axial and radial movements and high temperature gradients can cause excessive distortion of the sealing faces which may become amplified at large radii, high differential pressures and rotational speeds. Such distortions alter the geometry of the gap thereby affecting the seal's performance. This paper presents an extensive investigation into the air-film behaviour of a face seal under convergent and divergent engine representative coning distortions: 0.5 - 2 degrees, gap: 50 - 300 μm, and operating pressure differences 70 -350 kPa. The investigation approach is both numerical and experimental. Experimental tests allowed the introduction of a known distortion onto the static face of the seal. Arrays of static pressure tappings in the primary sealing gap were used to measure the radial and circumferential variations. The experimental data are used to validate a 3D CFD model of the primary leakage path. The CFD model was generated using ANSYS ICEM and solved using ANSYS FLUENT. The models were run at the full range of operating pressures and geometries.

1. Methods

A schematic outlining the main components of the experimental facility used in this study is shown in Figure 1.The rig consists of a baseplate on which is installed a rotating disc driven by an electric motor through a surface acoustic wave torque meter. The disc can be rotated at speeds of up to 15,000 rpm. The remaining key component of the test rig is the seal housing, which is connected to the baseplate via a load cell and electrically operated actuator. This allows displacement of the housing relative to the rotor of up to 4.1 mm to be applied in increments of 10 μm. The facility is installed in a pressure vessel allowing upstream pressurisation of the test rig. The seal housing is surrounded by high pressure air, with exhaust to atmospheric conditions through a secondary seal formed by a plane close fitting ring. Figure 2 shows a cross-sectional view of the sealing face installed within the seal housing. The primary leakage path of the flow is indicated with arrows. The sealing face geometry is machined onto a removable part which is an annulus is made from PVC (highlighted in orange in Figure 2). This allows different seal face gap profiles to be tested. The surface finish is essentially smooth in all cases. Thirteen radial pressure tappings are placed at each of ten circumferential locations (0°, 5°, 10°, 15°, 40°, 49°, 68°, 90°, 180° and 270°) around the annulus. In total, 130 pressure tappings provide sufficient

resolution to assess the pressure field within the sealing gap, and assess circumferential variation in the results. Please note that the geometric specifications of the test facility are not mentioned for proprietary reasons.

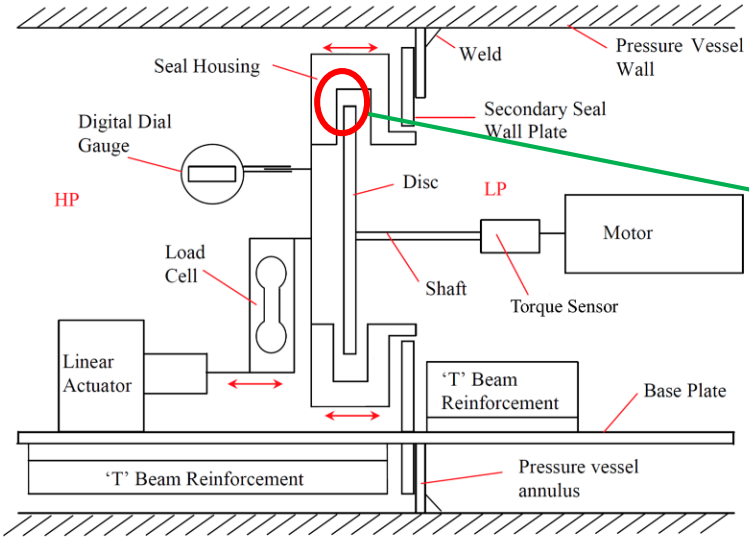

Figure 1 Non-Contacting Seals Rig Schematic.

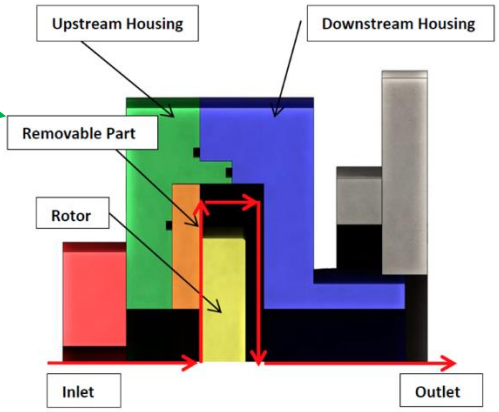

Figure 2 Leakage path.

2. Results

Figure 3 shows the circumferentially-averaged radial pressure distributions for three converging angles (α) at a minimum gap height ($\mathbf{h_{min}}$) of a 100 μm at an inlet pressure ($\mathbf{P_{in}}$) of 2.07 barg. The blue curve denoted by $\alpha = 0^o$ represents the corresponding parallel case for a given minimum gap height. In addition to experimental data, two dashed curves show the prediction obtained from solving a 1D compressible form of the Reynolds equation (**Eq.1**) for the parallel case and the largest converging angle case, $\alpha = -1.5^o$. Note that $\mathbf{r / |R^*|}$ is the normalised radial extent of the removable front face from the inner radius to the outer radius while the normalised radial pressure ($\mathbf{P(r)/P_{in}}$) is normalised by the inlet pressure**.** Figure 4 shows the radial pressure distributions for diverging gaps with a minimum gap height of 100 μm and two diverging coning angles ($\alpha = +1.0^o$ and $\alpha = +2.0^o$) at three inlet pressures. The plot highlights the effect of increasing the inlet pressure on the shock location and subsequent pressure recovery prior to the flow exiting the gap. All cases shown here are static tests.

$$\frac{\partial}{\partial x}\left(\frac{h^3}{\mu}\frac{\partial p^2}{\partial x}\right) = 0 \qquad \textbf{Eq. 1}$$

All cases showed an inertia-driven entry pressure loss which decreased with smaller gaps, the loss is due the flow taking a sharp corner just before entering the gap. For converging gaps, entry loss was more sensitive to the minimum gap height rather than the coning angle. Radial pressure distributions for converging configurations showed the highest air-film pressures and hence opening forces, which increased with an increase in converging angle. On the other hand, diverging gaps maintained the lowest air-film pressure out of all configurations. Additionally, radial pressure distributions from diverging cases uncovered a highly compressible behaviour involving choked flow conditions at the gap inlet and a supersonic flow region that was terminated by a series of shockwaves. The radial location of the minimum pressure moved further downstream at higher inlet pressures as higher Mach numbers were reached. This location showed little variation over the diverging angles tested for the same minimum gap. It was found to be more a function of inlet pressure and minimum gap height. For diverging gaps, entry loss increased as the minimum gap height increased, however, larger angles incurred a less severe loss in most cases. Contrary to the parallel and converging configurations where increasing the inlet pressure resulted in a desirable higher film pressure, it has proven to be detrimental to the film pressure where a diverging gap was present. More in-depth analyses and comparisons between the experimental data and the 3D CFD model will be presented in the final paper.

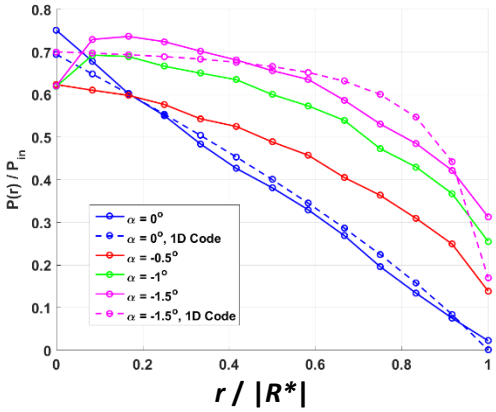

Figure 3 Experiments, Converging coning, Radial pressure distribution, h_{min} =100, P_{in}=2.07 barg.

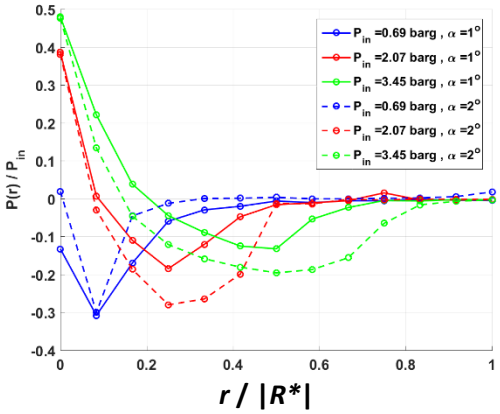

Figure 4 Experiments, Diverging coning, Radial pressure distribution, h_{min}=100μm, α = +1.0° and α = +2.0°.

References

[1] Ludwig, L.P., Gas Path Sealing in Turbine Engines, NASA TM–73890, 1978a.

[2] Munson, J., and Pecht, G., "Development of Film Riding Face Seals for a Gas Turbine Engine," Tribology Transactions 35, no. 1, January, 1992a.

[3] Steinetz, B.M., Hendricks, R.C., Munson, J., "Advanced Seal Technology Role in Meeting Next Generation Turbine Engine Goals," Propulsion and Power Systems First Meeting on Design Principles and Methods for Aircraft Gas Turbine Engines, sponsored by the NATO Research and Technology Agency, Toulouse, France, May 11–15, 1998, AVT-PPS Paper no. 11, NASA/TM-1998-206961, E-11109, May, 1998.

[4] Johnson, Robert L., and Ludwig, Lawrence P., Shaft Face Seal with Self-Acting Lift Augmentation for Advanced Gas Turbine Engines, NASA TN D-5170, 1969.